Thermal Properties of *t*-Butyl Nitrite (TBN) on Cu(111)

X.-M. Yan, M. D. Robbins, and J. M. White*

Department of Chemistry and Biochemistry, Center for Materials Chemistry, Texas Materials Institute, University of Texas, Austin, Texas 78712

Received: April 21, 2004; In Final Form: August 12, 2004

Reactions of coadsorbed *t*-butoxy and NO, generated by thermal dissociation of *t*-butyl nitrite dosed onto Cu(111), were investigated using time-of-flight mass spectrometry, temperature-programmed desorption, and Auger electron spectroscopy. In the high-temperature regime above 500 K, *t*-butyl alcohol, isobutene, carbon oxides, and molecular nitrogen desorb. In the more complex regime below 500 K, nitrous oxide, molecular nitrogen, hydrazine, water, carbon oxides, and acetylene desorb. The proposed low-temperature reaction pathways involve rearrangement of adsorbed nitric oxide to form N_2O and N_2, reaction between adsorbed $(CH_3)_3CO_{(a)}$ and $O_{(a)}$ or $N_{(a)}$ to form a metallocyclic intermediate (**1**) and either adsorbed $O_{(a)}H$ or $N_{(a)}H$. The intermediate (**1**) undergoes multiple C−C bond cleavages in a series of steps to form carbon oxides and adsorbed methylenes. The latter couple to form di-σ-bonded ethylene, which can either dehydrogenate to acetylene or be partially oxidized to acetate that dissociates in the high-temperature region. The proposed high-temperature *t*-butoxy decomposition is a bimolecular reaction involving transfer of hydrogen without forming chemisorbed H on Cu.

Introduction

Adsorbed alkoxy species are common intermediates in the heterogeneous partial oxidation of hydrocarbon molecules and are involved in several petrochemical processes.[1] Since β C−H bonds are 4−7 kcal/mol weaker than other C−H bonds, pyrolysis occurs mainly via β-hydrogen elimination when such H atoms are present.[2] The products are aldehydes or ketones on oxygen-covered metal surfaces.[3−6] Because it has no β-hydrogens, other pathways must be involved in the thermal decomposition of *t*-butoxy (TBO, $(CH_3)_3CO_{(a)}$, where the subscript a denotes the atom bound to Cu).[7−9] In a pioneering publication, Madix and co-workers first delineated these differences in a study of the surface chemistry of TBO on Ag(110).[10]

In ultrahigh vacuum (UHV) surface science studies, alkoxides are typically formed by dissociation of alcohols, for example, *tert*-butyl alcohol ($(CH_3)_3COH$, TBA). Relatively active group VIII transition metals, for example, Rh and Pt,[11] can activate this reaction at low temperature.[9,12−14] However, $O_{(a)}$ is typically required on Ag and Cu surfaces to promote dissociation; in the absence of $O_{(a)}$, the alcohol desorbs at temperatures below those required to activate O−H dissociation. For example, dissociation of TBA on Ag(110) requires coadsorbed oxygen to activate the transfer of H from the alcohol to form TBO and $O_{(a)}H$, a process that occurs well below 200 K.[10] During subsequent temperature-programmed desorption (TPD) of TBO and $O_{(a)}H$, the chemistry below 400 K is fully accounted for by $O_{(a)}H$ disproportionation to form $O_{(a)}$ and desorb H_2O. Above 400 K, the TBO and $O_{(a)}$ react to form and desorb several products including those requiring C−C bond cleavage, for example, acetone ($CH_3C(O)CH_3$) and CO_2. The CO_2 rate exhibits local maxima at two temperatures, 440 and 510 K. The rates of isobutylene oxide and isobutylene evolution also maximize at these two temperatures while the rate of TBA evolution is negligible at 440 K but maximizes at 510 K. To account for these products, two reaction paths were proposed—both involve an oxametallacycle intermediate.[10] The situation on Cu(110) differs from that on Ag(110): only one reaction path is required to account for a single maximum in the rates of isobutene and TBA desorption and there is no evidence for isobutylene oxide evolution.[7,15]

The requirement for coadsorbed $O_{(a)}$, places some stoichiometric constraints on the chemistry. First, the low-temperature $O_{(a)}H$/TBO ratio must equal 1 and the $(O_{(a)} + O_{(a)}H)$/TBO must be ≥ 1. Second, the $(O_{(a)} + O_{(a)}H)$/TBO ratio decreases when the low-temperature H_2O desorbs but can never fall below 0.5. Thus, the high-temperature reactions of TBO always occur in the presence of relatively large concentrations of $O_{(a)}$.

To probe other conditions, alkyl nitrites provide an alternative source of alkoxy species that do not require coadsorbed $O_{(a)}$. The relatively weak internal O−N bond (170 kJ/mol) makes dissociation at low temperatures facile even on relatively inactive surfaces.[8] On surfaces, for example, Ag(111), that do not readily activate this process, alkoxy formation can be achieved photochemically.[16] Provided the NO desorbs intact, as it does on Ag(111), a surface free of species other than the alkoxy can be realized. However, this condition is not fully realized on Cu(111) because NO dissociates. Still, $O_{(a)}$/TBO ratios lower than accessible when using TBA dosed on $O_{(a)}$-covered Cu(111) can be readily achieved with alkyl nitrite precursors.

Because NO is inherently involved, using nitrites is also of interest for modeling the reduction of NO_x, an important environmental issue. Surface science and catalytic research on NO_x reduction by hydrocarbons[17−19] has included metal oxides doped with oxidized Cu, Ag, and Au species.[20−22] These NO_x reduction events are accompanied by hydrocarbon oxidation, and alkoxy species are among likely intermediates.[23−25]

In the present work, we use time-of-flight mass spectrometry temperature-programmed desorption (TOFMS-TPD) and Auger electron spectroscopy (AES) to investigate the adsorption and thermal decomposition of *tert*-butyl nitrite (TBN, $(CH_3)_3CONO$) on Cu(111).

* Author to whom correspondence should be addressed.

10.1021/jp048259h CCC: $27.50
Published on Web 11/11/2004

Experimental Section

The apparatus has been described and comprises an ultrahigh vacuum chamber (UHV), base pressure of 3×10^{-10} Torr, equipped for time-of-flight mass spectrometry (TOFMS) and Auger electron spectroscopy (AES).[26] A Cu(111) crystal (MaTeck, 12 mm in dia and 2.5-mm thick) was mounted on a tungsten wire loop that, in turn, was connected to electrically isolated copper rods in the UHV system. The substrate was cooled to 85 K by contact with a liquid nitrogen reservoir and was resistively heated to temperatures as high as 900 K. Carbon, the primary surface contaminant, was removed by repeated cycles of 1.6 keV argon ion sputtering at 500 K and annealing for 10 min at 850 K. Surface cleanliness was verified by AES.

TBN (Aldrich, 90%), after several freeze−pump−thaw purification cycles, contained less than 2% TBA (mass spectrometry). TBN was dosed through a toggle-controlled, preset leak valve connected to a 3-mm ID tube that ended 2.5 cm from the copper surface. Before each dose, the pressure of the source connected to the toggle valve was set to 0.40 Torr (Baratron gauge). With this source pressure and no cooling of system surfaces, the leak valve was fixed to produce a chamber pressure increase of 1×10^{-8} Torr (measured by an ion gauge). In subsequent doses with the substrate cooled by connection to a liquid nitrogen reservoir, the leak valve remained fixed and the ion gauge was turned off to avoid electron-induced decomposition. Dosing was done by opening the toggle valve and stopped by closing it and simultaneously opening a valve to pump out the source. Relative exposures were calculated as pressure × dose time in Torr·second, assuming a constant flux of TBN determined by the 0.40 Torr pressure at the toggle valve. As described below, the exposures were normalized to unity at the maximum exposure that gives no intensity in the multilayer TPD peak.

Oxygen was used in several experiments and was dosed by backfilling through a separate leak valve to a chamber pressure of 1×10^{-6} Torr with the crystal held at 400 K**.** Oxygen coverages were calculated by comparing the measured oxygen-to-copper AES ratio with the saturation value, the latter set to 0.45 monolayer (ML), where 1 ML corresponds to 1 O atom per surface Cu atom.[27]

TPD was performed over the temperature range from 100 to 800 K with a ramp rate of 3.0 K s^{-1}. The temperature was measured with a type-K thermocouple inserted into a hole drilled into the top edge of the sample. During TPD, a full mass spectrum from 1 to 150 amu was acquired every 0.3 s. The upper limit exceeds the parent masses of TBA (74 amu) and TBN (103 amu), providing a data set searchable for desorption products containing up to eight carbons. Since every mass over the range is recorded in every scan, this method records in one experiment all the species that desorb and makes possible retrospective analysis for any positive ion within the mass range recorded.

Results

The results are summarized in two sets of TPD spectra (Figures1 and 4), one set of AES spectra (Figure 2), and a peak area summary, Figure 3. Figures 1 and 2 compare TPD and AES for 4 exposure unit (EU, defined below) doses of TBN on clean Cu(111) at 100 K; Figure 3 summarizes TPD for TBN doses between 0 and 5 EU on clean Cu(111), and Figure 4 is TPD for a 4 EU dose of TBN on O-covered Cu(111).

From the 150 masses scanned and analyzed, the eight shown in Figure 1 were selected to indicate the complete set of desorbing products. All other masses either showed no intensity or were fragments of a product identified from Figure 1. There is a peak at 143 K for every ion shown as well as for the 30 and 88 amu signals (not shown). These are all attributed to TBN multilayer desorption as observed on Rh (145 K)[14] and Pt (150 K).[9] Toward higher temperature, there was no evidence for distinct molecular desorption features indicating that TBN in contact with copper either dissociates during dosing or subsequent TPD or is displaced during TPD by nearby TBN dissociation. Arbitrarily defining 1 EU as the largest dose (not shown) that does not give the multilayer peak at 143 K and assuming a constant sticking coefficient, the dose of Figure 1 is 4 EU. Anticipating the discussion, the TPD data fall into two temperature regimes—above and below 500 K.

Other than those at 143 K, the peaks in Figure 1 are assigned, on the basis of fragmentation pattern analysis, to 10 molecules.

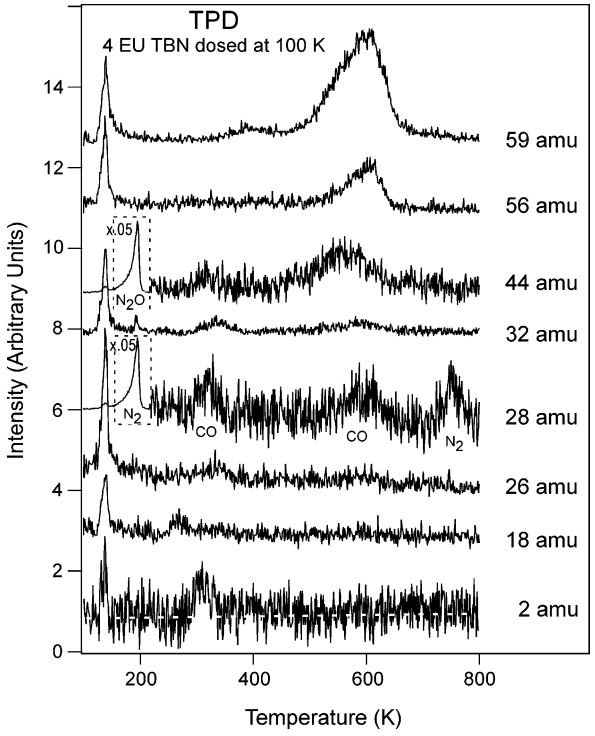

Figure 1. TOFMS-TPD (3.0 K s^{-1}) of 4 EU (exposure units) of *t*-butyl nitrite (TBN) dosed onto clean Cu(111) at 100 K. The traces of 28 and 44 amu between 100 and 220 K (dashed rectangles) are scaled by 0.05.

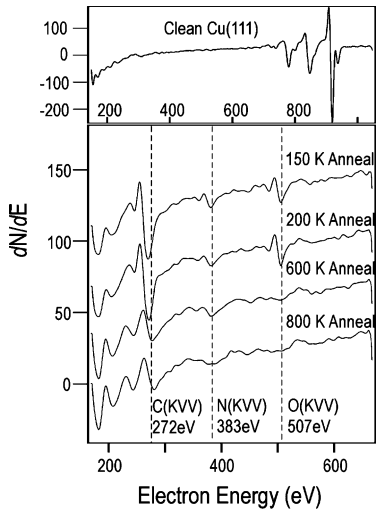

Figure 2. Upper panel: AES of a clean Cu(111) surface. Bottom panel: AES of 4 EU TBN on Cu(111) annealed to different temperatures. All spectra were taken at 150 K after annealing for 60 s at the indicated temperature. To minimize electron-induced effects,[31] each spectrum was taken at a different physical location.

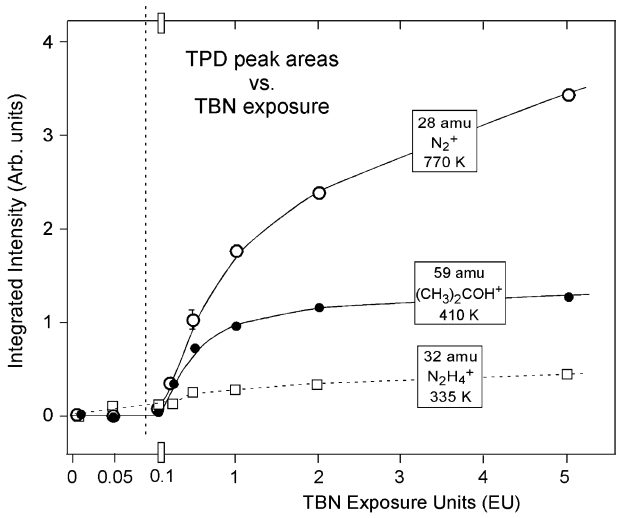

Figure 3. Selected TPD peak areas as a function of TBN dose in exposure units (EU) on Cu(111) at 100 K. The peaks are identified by the peak temperatures indicated on each curve. To emphasize the onset of these three peaks, an expanded scale from 0 to 0.1 EU is used.

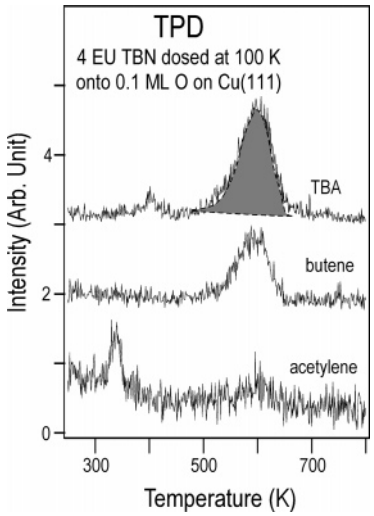

Figure 4. TOFMS-TPD of 4 EU TBN dosed onto oxygen-covered (θ = 0.1 ML) Cu(111) at 100 K. Compared to TBN on clean Cu(111) (Figure 1), more acetylene forms. A scaled isobutene signal ($\times$1.7) is shown as the darkened region superimposed on the 600 K TBA desorption peak. The fit is excellent except for the low-temperature shoulder region of the TBA profile (see text).

From bottom to top, the assignments are 2 amu, dihydrogen; 18 amu, water; 26 amu, acetylene; 28 amu, carbon monoxide and dinitrogen; 32 amu, hydrazine; 44 amu, carbon dioxide and nitrous oxide; 56 amu, isobutene; and 59 amu, TBA. We found no evidence for any C_2 hydrocarbons other than acetylene.

Before discussing these somewhat complex TPD spectra in terms of the surface species leading to the desorbing products, it is useful to consider the AES spectra found after annealing to selected temperatures, Figure 2. Annealing to 150 K, just above the TBN desorption temperature, leaves C-, N-, and O-containing species. The results are typical of sp^3 hybridized carbon;[28,29] there is 14 eV between the maximum of the positive-going excursion and the minimum of the negative-going excursion of the C KVV signal. Annealing to 200 K decreases the N and O AES signals slightly, but C is unchanged. This is consistent with the desorption of N_2O and N_2 (Figure 1) in this region. Annealing to 600 K reduces the N and C AES signals, and, importantly, the O signal becomes undetectable. The C signal broadens (to 16 eV) and shifts to higher kinetic energy (272 eV) reflecting a significant contribution of sp^2 hybridization consistent with dehydrogenation and rearrangement of *t*-butoxy species as expected from TPD. Annealing to 800 K reduces the N signal below detectability while the C signal remains relatively intense. Loss of the N(KVV) signal is consistent with desorption of N_2 peaking at 750 K (Figure 1) where recombination of $N_{(a)}$ occurs.[30] The C(KVV) AES profile is consistent with sp^2 hybridization, that is, oligomerized graphitic carbon.

While the AES profiles reflect neither detailed chemical structures nor their evolution as the annealing temperature increases, the measured surface atomic compositions and the C(KVV) line shapes can guide the construction of reaction path models. Clearly, any acceptable mechanism must account for the retention of significant amounts of carbon at 800 K, the conversion from sp^3 to sp^2 hybridized carbon between 200 and 600 K, the loss of $O_{(a)}$ at $\sim$600 K, the presence of significant amounts of $N_{(a)}$ from 150 to 600 K, and the loss of $N_{(a)}$ between 600 and 800 K.

With these TPD-AES correlations in mind, we return to information supporting the TPD assignments. The sharp 44 and 28 amu peaks at 194 K are assigned as a mixture of N_2O (44 amu) and N_2 (28 amu) since the 28-to-44 amu ratio is very close to unity, far removed from the fragmentation ratio (0.11) measured for N_2O. Thus, upon reaching 200 K, the evidence points to a surface covered with a mixture of $N_{(a)}$, $O_{(a)}$, and TBO. Assuming the mass spectrometer sensitivity factors for N_2O at 44 amu and N_2 at 28 amu are roughly equal, and that very little NO desorbs, the estimated $O_{(a)}$-to-TBO at 200 K is 0.76. As expected, since some N_2O desorbs, this value is less than unity. The 18 amu peak at 265 K is assigned to H_2O formed in a reaction-limited process that, revealingly, requires C−H bond breaking, that is, some dehydrogenation of CH_3 groups of $(CH_3)_3CO_{(a)}$.

When the H_2O desorption rate starts to fall, dehydrogenation does not stop since H_2 desorption commences (Figure 1). Evidently, the concentration of either $O_{(a)}$ or $O_{(a)}H$ becomes so small, at least for this dose and in this temperature region, that the rate of H_2O formation is no longer competitive. The H_2 desorption rate peaks at 310 K. While simple second-order kinetics would exhibit a desorption profile that is less symmetric than observed, no unambiguous conclusion about the kinetics can be drawn since the high concentration of coadsorbed species likely influences the effective kinetic order of the H_2 formation and desorption path.

In addition to the C−H bond breaking required for H_2O desorption, C−C bond breaking is required to account for the CO and CO_2 (28 and 44 amu) peaks at 320 K. While these two peaks track each other from 290 to 350 K, the I_{44}/I_{28} intensity ratio is too low to suggest 100% CO_2. The kinetics are reaction limited since 320 K lies well above desorption from Cu(111) of either adsorbed molecular CO (170 K)[32] or CO_2 (200 K).[33] The faithful tracking suggests a common intermediate leading to CO and CO_2. The barely visible 26 amu peak at 335 K is assigned to acetylene and was stronger when coadsorbed O(a) was involved (see Figure 4 below). At 390 K, there is a weak 59 amu peak assigned to TBA formed by hydrogenation of TBO. Evidently, above 310 K, there is a source of H, even though the H_2 signal drops and the $O_{(a)}H$ has been consumed.

In this regard, the 32 amu profile in the region just above 300 K is interesting. On the basis of the analysis of numerous ion signals and several doses of TBN (see below), the 335 K peak in 32 amu is assigned to hydrazine, $N_2H_4^+$, a feature consistent with $N_{(a)}$ being active in the C−H dehydrogenation pathway, that is, we propose that $N_{(a)}$ catalyzes the cleavage of

SCHEME 1: Thermal Decomposition, *t*-Butoxy Coadsorbed with O(a) and N(a), Reactions Involving C-Containing Species

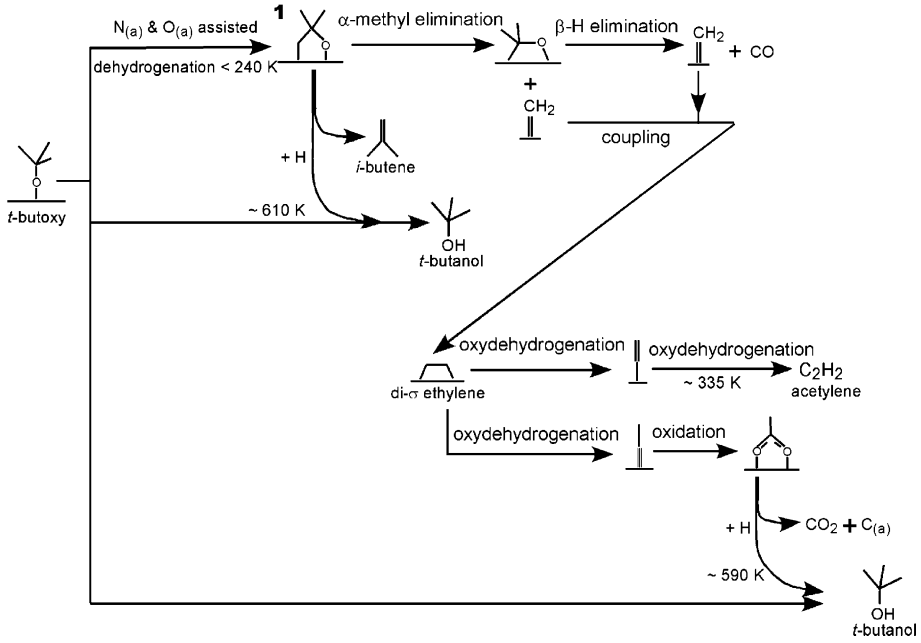

C−H bonds in TBO to form $N_{(a)}H_x$ ($x = 1, 2$), the latter serving as both the H source to form TBA from TBO at 390 K and as the source of the N_2H_4 desorption peak at 335 K.

Moving to higher temperature (490 K), the coincident onsets of 44 and 59 amu (CO_2 and TBA) are consistent with hydrogen transfer from TBO to a nearby TBO, that is, a bimolecular process, perhaps mediated by $N_{(a)}$, to desorb TBA and CO_2 and leave a H-deficient activated species that desorbs as isobutene at slightly higher temperatures.

By 680 K, all desorption signals, except for 28 amu, have returned to background levels, that is, C−H bonds are no longer breaking. The highest temperature 28 amu peak is attributed to the $N_{(a)}$ recombination (760 K)[34] and is also confirmed by AES annealing results (Figure 2). For very low TBN doses, the available $N_{(a)}$ is consumed by other paths since no N_2 desorbs in this temperature region (Figure 3). This is consistent with the proposed formation of $N_{(a)}H_x$. As noted above, AES after the sample was heated to 800 K shows the $N_{(a)}$ signal has fallen below the AES detection limit (<0.01 ML) while the residual C signal is strong (Figure 2).

As the exposure of TBN increases from 0 to 5 EU, the integrated areas of selected peaks—the 770 K (N_2, 28 amu), 410 K (TBA, 59 amu), and 335 K (N_2H_4, 32 amu)—exhibit interesting properties (Figure 4). From the origin to 0.1 EU, an expanded *x*-axis is used to emphasize that measurable desorption in the 770 K N_2 peak does not occur for exposures less than 0.1 EU. On the other hand, there is measurable intensity in the 335 K N_2H_4 peak even at 0.05 EU. Above 0.1 EU, the 410 K (TBA) and 335 N_2H_4 peaks maintain a constant ratio of 3 while the 770 K N_2 peak grows monotonically. At some exposure, this peak should saturate but that situation was not realized here.

Additional insight was gained by TPD (Figure 4) after dosing 4 EU of TBN on a surface precovered with 0.1 ML of O prepared by dosing O_2 and measuring the AES spectrum (not shown). Compared to Figure 1, the 26 amu peak (C_2H_2) at 335 K is more intense while the 56 and 59 peaks retain their relative intensities and positions. Except for the low-temperature side where there is a shoulder on the 59 amu signal, a scaled version of the 56 amu peak overlaps the 59 amu peak pointing to a reaction that produces both species from a common intermediate. The shoulder is clearer in the data of Figure 1.

Discussion

It is clear from the results that, while the chemistry of TBN on Cu(111) is relatively complex, several reaction pathways are supported. The desorption of N_2O and N_2 at 200 K is in accord with the behavior of NO on coinage metal surfaces; dimerization to form $(NO)_2$ followed by rearrangement is well known. [35] After N_2O desorption at 200 K, $O_{(a)}$, $N_{(a)}$, and $TBO_{(a)}$ will remain. Scheme 1 summarizes a set of reactions, limited to the C-containing species, that are consistent with our observations.

Above 200 K, the desorption of H_2O requires a source of hydrogen, that is, C−H bond breaking, most likely through dehydrogentation of TBO by reaction with $O_{(a)}$ or N(a) derived from NO to form $HO_{(a)}$ or $HN_{(a)}$ species that recombine to form H_2O at 265 K.[36,37] Since reaction of $H_{(a)}$ with $O_{(a)}$ is not observed on Cu(111),[38] we propose $HO_{(a)}$ is formed either through an interaction with $O_{(a)}$ of C−H or $HN_{(a)}$. Either route leads to dehydrogenation of TBO. The H_2O peak at 265 K is attributed to a reaction-limited process since adsorbed molecular water desorption from Cu(111) is complete by 190 K. [39,40]

For our conditions, the desorption of N_2O and NO implies that above 200 K the concentration ratio, $[HO_{(a)}]/[TBO(a)]$, is persistently lower, as expected, compared to a situation where TBO is coadsorbed with $O_{(a)}$ on Cu(110). On Cu(110), dosed H_2O desorbs below 200 K[41] and for TBA dosed onto $O_{(a)}$, H_2O desorption appears with two peaks below 500 K (270 and 330 K).[7,15] While only the 330 K peak was originally interpreted as reaction-limited, we interpret both as falling into this category.

The decay of the H_2O signal and the simultaneous rise of the H_2 signal is striking. While there is still oxygen in remaining TBO, the $O_{(a)}$ from $NO_{(a)}$ dissociation has been consumed. There is continued activation of C−H bonds or N−H bonds, since C−H dehydrogenation evidently produces $H-N_{(a)}$ that, among other paths, leads to N_2H_4 desorption. These sources supply H for the H_2 desorbing at 310 K.

Low-temperature C−H activation is clearly required to rationalize our results. In the absence of coadsorbed species, C−H activation leading to $H_{(a)}$ bound to Cu is not facile on

Cu(111). For example, $C_{(a)}H_3$ on Cu(111) is stable up to 400 K[42] and TBO on Cu(110)[7,15] and Cu(111) is stable to between 500 and 600 K.[8] We propose that $O_{(a)}$ and $N_{(a)}$ are involved in the dehydrogenation of TBO and facilitate the chemistry observed between 240 and 360 K. As indicated in Scheme 1, an oxymetallacycle intermediate (**1**) proposed in earlier work[7,15]

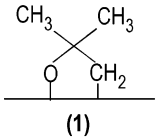

(1)

is an attractive candidate that could be formed by interaction of CH_3 from TBO with adjacent $N_{(a)}$ or $O_{(a)}$. The resulting $O_{(a)}H$, formed below 240 K, can account for the H_2O that desorbs at higher temperatures while the $N_{(a)}H$ either decomposes to $N_{(a)}$ and $H_{(a)}$, accounting for the H_2 that forms, or hydrogenates further to form hydrazine that desorbs at 335 K.

Once **1** forms and the $O_{(a)}$ derived from NO dissociation has been consumed to form H_2O, the adsorbates will include $N_{(a)}$, and the oxygenates, **1** and TBO. The decomposition of **1** can account for the products that desorb between 300 and 400 K, namely, CO, CO_2, and C_2H_2. Following Scheme 1, we propose that **1** loses methyl groups, facilitated by $N_{(a)}$, to form methylene, $C_{(a)}H_2$, groups that couple to form di-σ-bonded ethylene. The latter dehydrogenates to form either ethylidyne, $\equiv C_{(a)}CH_3$, or acetylene, $HCCH_{(g)}$, via a vinyl intermediate, $-C_{(a)}H{=}CH_2$. The ethylidyne is unreactive until high temperatures ($\sim$590 K) are reached. Desorption of CO and CO_2 requires C$-$C bond cleavage and likely involves decarbonylation or decarboxylation of oxygenates, $CH_xCO_{y(a)}$, consistent with C_2H_2 desorption in the same temperature region. The desorption of both CO and CO_2 sets in at slightly higher temperatures than H_2, but all three decay away with the same thermal profile.

The formation of acetylene is very interesting.[43,44] Low-temperature alkyl C$-$C cleavage without oxidation has been reported for neopentyl groups $(CH_3)_3CC_{(a)}H_2$, adsorbed on Ni(100).[45,46] The process involves methyl elimination to form isobutene (C_4H_8) and methylene, $C_{(a)}H_2$, at or below 200 K. If TBO undergoes low-temperature dehydrogenation to form species **1**, there will be methyl groups in the analogous position. Methyl elimination from **1** would yield surface methylene and a rearranged adsorbed species, either dimethyl methyleneoxy (**2**) or di-σ-dimethyl methoxy (**3**), Scheme 2. The latter is favored since **2** is expected to lead to acetone which is not observed. Intermediate **3** can oxydehydrogenate, eliminate the two remaining methyl groups via the commonly observed β-H elimination pathway, and generate $CO_{(a)}$, $OH_{(a)}$, and $C_{(a)}H_2$.

SCHEME 2: Proposed Intermediates, TBO Decomposition below 300 K

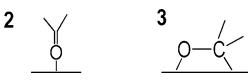

Under our conditions, an attractive route to acetylene involves adsorbed methylene, a well-studied adsorbate.[46,47] Coupling to form and desorb ethylene is typical on copper but for our case, we suppose $C_{(a)}H_2$ either couples to $H_2C_{(a)}C_{(a)}H_2$, di-σ ethylene,[47] followed by rearrangement to acetylene or methylene dehydrogenation to methylidyne, $CH_{(a)}$, that couples to acetylene. Methylene chemistry on copper[48$-$50] indicates that coupling and oxidation (including oxydehydrogenation and dehydrogenation) compete. Dehydrogenation to methylidyne, $C_{(a)}H$ and $H_{(a)}$, although dominant on group VIII transition metals, is not common on coinage metals.[46] Furthermore, methylidyne coupling to acetylene, reported to occur on Ni(111),[51] has not been reported on Cu. These considerations lead us to favor di-σ-bonded ethylene as the precursor to acetylene. In competition, di-σ-bonded ethylene can dehydrogenate to ethylidyne, $CH_3C_{(a)}$, at 370 K.[47] Alternatively, ethylene could react with surface oxygen on Cu(111) to form acetylene as follows:[37,52]

$$C_2H_{4(a)} + O_{(a)} \rightarrow HC_{(a)}C_{(a)}H_2 + HO_{(a)}$$

$$HC_{(a)}C_{(a)}H_2 + O_{(a)} \rightarrow C_2H_2(a) + HO_{(a)}$$

However, methylene conversion to acetylene by coupling and oxydehydrogenation is not the only plausible reaction path. As noted earlier, the TBA desorption peak at 590 K has a shoulder on the lower temperature side coincident with the CO_2 peak (Figure 1). The TBA shoulder becomes a separate peak and is clearly resolved at lower TBN exposures (not shown). Comparing 4 EU TBN dosed onto oxygen-covered ($\theta = 0.1$) Cu(111) (Figure 4) to the same amount of TBN onto clean Cu(111) (Figure 1), the TBA and isobutene desorption peaks track each other, except for the leading edges where a reaction transferring hydrogen to TBO is still occurring. The acetylene intensity increases as the 580 K TBA shoulder decreases, indicating the reaction pathway leading to the acetylene competes with the pathway leading to the intermediate that forms the TBA responsible for the 580 K shoulder.

To identify the intermediate, careful study of Figure 1 from 520 to 560 K is necessary. Between the onset of TBA and the onset of isobutene, the only desorbing species besides TBA is CO_2, indicating the intermediate is an O-containing species. To form TBA from TBO, one additional hydrogen is needed. Thus, the intermediate also contains H. No CO desorbs during this process consistent with the two oxygen atoms used to form CO_2 being bonded to the same carbon in the intermediate, that is, the intermediate has a carboxylate ($RCO_{(a)}O_{(a)}^-$) or dioxy (R_1R_2-$CO_{(a)}O_{(a)}$) form. The former is favored since dioxy is unstable and decomposes at very low temperature, for example, η^2-methylenedioxy decomposes at 225 K on Ag(110).[53] The simplest carboxylate, formate, is excluded since surface formate ($HCOO^-$) decomposes at much lower temperature$-$480 K on Cu(111)[54] and 460 K on Cu(110).[55] Acetate is an attractive candidate; on Cu(110) it decomposes at $\sim$590 K.[56,57]

At least two possible pathways exist for the proposed di-σ-bonded ethylene. One is partial oxidation, likely via the ethylidyne intermediate, to form acetate, that decomposes at 590 K. The other, as envisioned in Scheme 3, involves a vinyl

SCHEME 3: Proposed Mechanism of Acetylene Formation from Methylene via a Vinyl Intermediate

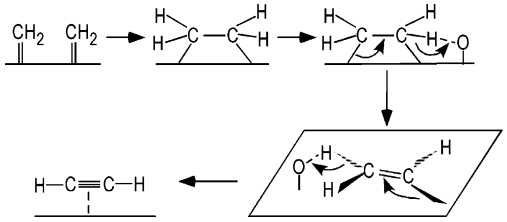

intermediate[58] and forms acetylene that desorbs at 335 K (Figure 1). If $O_{(a)}$ is present, as it is under the conditions of Figure 4, the vinyl pathway is favored, probably because of the electron-withdrawing effect induced by coadsorbed oxygen. In the absence of $O_{(a)}$, ethylidyne formation is favored. We propose an intramolecular hydrogen transfer from di-σ-bonded ethylene to form ethylidyne. During this process, the hydrogen becomes

transiently acidic and readily transfers to $O_{(a)}$. Thus, what starts as an intramolecular hydrogen transfer becomes an intermolecular proton transfer, that is, oxydehydrogenation to form a vinyl group.

A relation between N_2 desorption and the weak 410 K TBA desorption is supported by the results shown in Figure 3. The desorption of both N_2 and this low T portion of TBA sets in at the same TBN exposure and the trends track each other. For low exposures (<0.1 EU), there is neither 770 K N_2 nor 410 K TBA, but the 335 K N_2H_4 peak is present. When the exposure increases to 0.25 EU, the 770 K N_2 peak appears along with the TBA peak at 410 K. Above 410 K, the proposed surface species are acetate that decomposes at 580 K, TBO that decomposes at 600 K, C_nH_m, and N_xH_y. Some of the hydrogen-deficient C_nH_m reacts with oxygen to form CO at 600 K while the residual remains up to at least 800 K. The N_xH_y is attractive as a precursor to N_2H_4 and H_2 at lower temperatures and as an intermediate that facilitates H-transfer reactions at higher temperature. In this regard, $NH_{x(a)}$ ($x = 1, 2$) has been reported when ammonia is oxidized by O_2 or NOX and has been identified spectroscopically on many metal surfaces, including copper.[37,59,60]

Finally, while there are many similarities between TBN on Cu(111) and TBA on O-covered Cu(110), there are differences, particularly in the low-temperature region (<300 K). TBO formed from TBA dosed on O-covered Cu(110) does not react to form C2 species as it does on Cu(111).

Summary

A TOFMS-TPD and AES investigation of *t*-butyl nitrite (TBN, $(CH_3)_3CO-NO$) on Cu(111) leads to the following conclusions. During adsorption at 110 K and during subsequent TPD, the internal N−O bond breaks to form *t*-butoxy (TBO, $(CH_3)_3CO_{(a)}-$) and NO. NO decomposes, some forming N_2O and N_2 that desorb together at 194 K, and some leaving $N_{(a)}$ and $O_{(a)}$ that play important roles in facilitating C−H bond cleavage. Some TBO decomposes at fairly low temperature (<240 K) to form water, carbon monoxide, carbon dioxide, and acetylene that desorb and NH_x and acetate that are adsorbed. The remaining TBO disproportionates to form *t*-butyl alcohol and isobutene at 600 K. The proposed low-temperature TBO reactions are limited by C−H cleavage. The breaking of C−H bonds is followed by C−C rupture to form adsorbed methylene. The methylene couples to di-σ-bonded ethylene that either dehydrogenates to acetylene desorbing at 335 K via a vinyl intermediate or is partially oxidized to acetate that dissociates at 580 K. There is also evidence for NH bond formation and N_2H_4 desorption during this process. The high-temperature *t*-butoxy decomposition is consistent with a bimolecular reaction involving intermolecular hydrogen transfer.

Acknowledgment. The authors acknowledge support by the Chemical Sciences, Geosciences and Biosciences Division, Office of Basic Energy Sciences, Office of Science, U.S. Department of Energy and by the Robert A. Welch Foundation (F-0032).

References and Notes

(1) Weissermel, K.; Arpe, H.-J. *Industrial Organic Chemistry*, 3rd ed.; Weinheim: New York, 1997.
(2) Weldon, M. K.; Friend, C. M. *Chem. Rev.* **1996**, *96*, 1391−1411.
(3) Bowker, M.; Madix, R. J. *Surf. Sci.* **1980**, *95*, 190−206.
(4) Bowker, M.; Madix, R. J. *Surf. Sci.* **1982**, *116*, 549−72.
(5) Davis, J. L.; Barteau, M. A. *Surf. Sci.* **1987**, *187*, 387−406.
(6) Ali, A. H.; Zaera, F. *J. Mol. Catal., A* **2002**, *177*, 215−235.
(7) Brainard, R. L.; Madix, R. J. *J. Am. Chem. Soc.* **1989**, *111*, 3826.
(8) Ihm, H.; Scheer, K.; Celio, H.; White, J. M. *Langmuir* **2001**, *17*, 786−790.
(9) Ihm, H.; Medlin, J. W.; Barteau, M. A.; White, J. M. *Langmuir* **2001**, *17*, 798−806.
(10) Brainard, R. L.; Madix, R. J. *J. Am. Chem. Soc.* **1987**, *109*, 8082−8083.
(11) Bol, C. W. J.; Friend, C. M. *Surf. Sci.* **1996**, *364*, L549.
(12) Xu, X.; Friend, C. M. *Langmuir* **1992**, *8*, 1103.
(13) Xu, X.; Friend, C. M. *J. Phys. Chem.* **1991**, *95*, 10753.
(14) Yan, X.-M.; Kim, C.; White, J. M. *J. Phys. Chem.* **2001**, *105*, 3587−3593.
(15) Brainard, R. L.; Madix, R. J. *Surf. Sci.* **1989**, *214*, 396.
(16) Zhao, W.; Kim, C.; Kim, S. K.; White, J. M. *J. Phys. Chem. A* **2001**, *105*, 2234−2239.
(17) Shelef, M. *Chem. Rev.* **1995**, *95*, 209−225.
(18) Jang, B. W. L.; Spiver, J. J.; Kung, M. C.; Yang, B.; Kung, H. H. *ACS Symposium Series* **1995**, *587*, 83−95.
(19) Burch, R.; Breen, J. P.; Meunier, F. C. *Appl. Catal., B* **2002**, *39*, 283−303.
(20) Konin, G. A.; Il'ichev, A. N.; Matyshak, V. A.; Khomenko, T. I.; Korchak, V. N.; Sadykov, V. A.; Doronin, V. P.; Bunina, R. V.; Alikina, G. M.; Kuznetsova, T. G.; Paukshtis, E. A.; Fenelonov, V. B.; Zaikovskii, V. I.; Ivanova, A. S.; Beloshapkin, S. A.; Rozovskii, A. Y.; Tretyakov, V. F.; Ross, J. R. H.; Breen, J. P. *Top. Catal.* **2001**, *16/17*, 193−197.
(21) Kung, M. C.; Bethke, K. A.; Yan, J.; Lee, J.-H.; Kung, H. H. *Appl. Surf. Sci.* **1997**, *121/122*, 261−266.
(22) Nyarady, S. A.; Sievers, R. E. *J. Am. Chem. Soc.* **1985**, *107*, 3726−7.
(23) Kameoka, S.; Ukisu, Y.; Miyadera, T. *Phys. Chem. Chem. Phys.* **2000**, *2*, 367−372.
(24) Haneda, M.; Kintaichi, Y.; Inaba, M.; Hamada, H. *Bull. Chem. Soc. Jpn.* **1997**, *70*, 499−508.
(25) Montreuil, C. N.; Shelef, M. *Appl. Catal.* **1991**, *75*, L1.
(26) Kim, C.; Yan, X. M.; White, J. M. *Rev. Sci. Instrum.* **2000**, *71*, 3505.
(27) Habraken, F. H. P. M.; Kieffer, E. P.; Bootsma, G. A. *Surf. Sci.* **1979**, *83*, 45−59.
(28) Lascovich, J. C.; Giorgi, R.; Scaglione, S. *Appl. Surf. Sci.* **1991**, *47*, 17−21.
(29) Patsalas, P.; Handrea, M.; Logothetidis, S.; Gioti, M.; Kennou, S.; Kautek, W. *Diamond Relat. Mater.* **2001**, *10*, 960−964.
(30) Madix, R. J. *Surface Reactions*; Springer-Verlag: New York, 1994; Vol. 34.
(31) Lee, I.; Kim, S. K.; Zhao, W.; White, J. M. *Surf. Sci.* **2002**, *499*, 53−62.
(32) Kirstein, W.; Kruger, B.; Thieme, F. *Surf. Sci.* **1986**, *176*, 505−529.
(33) Fu, S. S.; Somorjai, G. A. *Langmuir* **1992**, *8*, 518−524.
(34) Berko, A.; Solymosi, F. *Appl. Surf. Sci.* **1992**, *55*, 193−202.
(35) Brown, W. A.; King, D. A. *J. Phys. Chem. B* **2000**, *104*, 2578−2595.
(36) Au, C.-T.; Breza, J.; Roberts, M. W. *Chem. Phys. Lett.* **1979**, *66*, 340−344.
(37) Au, C. T.; Roberts, M. W. *Chem. Phys. Lett.* **1980**, *74*, 472−474.
(38) Kammler, T.; Kuppers, J. *J. Phys. Chem. B* **2001**, *105*, 8369−8374.
(39) Hinch, B. J.; Dubois, L. H. *J. Chem. Phys.* **1992**, *96*, 3262−3268.
(40) Theil, P. A.; Madey, T. E. *Surf. Sci. Rep.* **1987**, *7*, 211−385.
(41) Clendening, W. D.; Rodriguez, J. A.; Campbell, J. M.; Campbell, C. T. *Surf. Sci.* **1989**, *216*, 429−461.
(42) Chuang, P.; Chan, Y. L.; Chien, S.-H.; Song, K.-J.; Klauser, R.; Chuang, T. J. *Langmuir* **2002**, *18*, 4549−4552.
(43) Outka, D. A.; Friend, C. M.; Jorgensen, S.; Madix, R. J. *J. Am. Chem. Soc.* **1983**, *105*, 3468−3472.
(44) Avery, N. R. *J. Am. Chem. Soc.* **1985**, *107*, 6711−6712.
(45) Zaera, F.; Tjandra, S. *J. Am. Chem. Soc.* **1993**, *115*, 5851−5852.
(46) Bent, B. E. *Chem. Rev.* **1996**, *96*, 1371.
(47) Solymosi, F. *J. Mole. Catal., A* **1998**, *131*, 121−133.
(48) Lin, J.-L.; Chiang, C.-M.; Jenks, C. J.; Yang, M. X.; Wentzlaff, T. H.; Bent, B. E. *J. Catal.* **1994**, *147*, 250.
(49) Chiang, C.-M.; Bent, B. E. *Surf. Sci.* **1992**, *289*, 79.
(50) Shustorovich, E.; Bell, A. T. *Surf. Sci.* **1991**, *248*, 359.
(51) Yang, Q. Y.; Maynard, K. J.; Johnson, A. D.; Ceyer, S. T. *J. Chem. Phys.* **1995**, *102*, 7734.
(52) Kovacs, I.; Solymosi, F. *J. Mole. Catal., A* **1999**, *141*, 31.
(53) Stuve, E. M.; Madix, R. J.; Sexton, B. A. *Surf. Sci.* **1982**, *119*, 279−90.
(54) Russell, J. N., Jr.; Gates, S. M.; Yates, J. T., Jr. *Surf. Sci.* **1985**, *163*, 516−540.
(55) Bowker, M.; Madix, R. J. *Surf. Sci.* **1981**, *102*.
(56) Bowker, M.; Madix, R. J. *Appl. Surf. Sci.* **1981**, *8*.
(57) Surman, M.; Lackey, D.; King, D. A. *J. Electron Spectrosc. Relat. Phenom.* **1986**, *39*, 245−254.
(58) Yang, M. X.; Eng, J., Jr.; Kash, P. W.; Flynn, G. W.; Bent, B. *J. Phys. Chem.* **1996**, *100*, 12431−12439.

(59) Matloob, M. H.; Roberts, M. W. *J. Chem. Soc., Faraday Trans.* **1997**, *73*, 1393.

(60) Asfin, B.; Davies, P. R.; Pashuski, A.; Roberts, M. W. *Surf. Sci* **1991**, *259*, L724-L728.